Digest Journal of Nanomaterials and Biostructures Vol. 6, No 1, January-March 2011, p. 451-466

INFLUENCE OF Tl^+ DOPING ON OPTO-STRUCTURAL AND ELECTRICAL PROPERTIES OF CHEMICALLY GROWN TUNGSTEN HETEROPOLYOXOMETALATE THIN FILMS

S. R. MANE[a,*] R. R. KHARADE[b], R. M. MANE[b], S.N.GAWALE[b], S.M. PATIL[b], P. N. BHOSALE[b]

[a]*Department of Chemistry, K. R. Patil Kanya Mahavidyalaya, Islampur, 415409, Maharashtra, India*

[b]*Materials Research Laboratory, Department of Chemistry, Shivaji University, Kolhapur. 416004, Maharashtra, India*

In present investigation, thin films of tungsten heteropolyoxometalates viz. undoped phosphotungstic acid [$H_3 (PW_{12} O_{40})$] and Tl^+ doped phosphotungstic acid [$Tl_3 (PW_{12} O_{40})$] were deposited at optimum deposition conditions by chemical growth process using organic and aqueous solutions of phosphotungustic acid and thallous acetate respectively. In this study, the optostructural and electrical properties of undoped and Tl^+ doped tungsten heteropolyoxometalate thin films have been studied by scanning electron microscopy (SEM), atomic force microscopoy (AFM), X-ray diffraction, optical absorption, dc electrical resistivity and thermo-electric power techniques. Morphological study performed on scanning electron microscopy and atomic force microscopy shows after doping Tl^+ there is formation of spherical shaped grains of $Tl_3 (PW_{12} O_{40})$ heteropolyoxometalate . X-ray diffraction study revealed that, the material is polycrystalline in nature having simple cubic spinel structure. After doping Tl^+, intensity of prominent peak (311) increases and other peaks are suppressed, indicating intercalation of Tl^+ in the octahedral lattice of phosphotungstate anion without change in crystal structure. The optical absorption study revealed that, there is decrease in band gap (Eg) of material after doping Tl^+. DC electrical resistivity measurement study shows, after doping Tl^+ the heteropolyoxometalate material $Tl_3 (PW_{12} O_{40})$ shows semiconducting behavior at lower temperature. The TEP study shows, generated voltage possesses plus sign over the whole range of temperature providing p-type semiconducting behavior. The TGA-DTA study revealed that, after doping Tl^+, stability of $Tl_3 (PW_{12} O_{40})$ material increases and the material is thermally stable up to 265.12 °C.

(Received November 22, 2010; accepted January 5, 2011)

Keywords: Thin films, Chemical synthesis, Crystal structure, Thermoelectrical, Tl-doping, TGA-DTA, Atomic force microscopy (AFM)

1. Introduction

Heteropolyoxometalate (HPOM) has been a matter of interest in basic and applied science for more than a century. From their first synthesis, many advances have been made to promote the use of HPOM in different ways in science and technology. The applications of HPOM are associated with their interesting properties such as anionic size, high ionic weight, high redox characteristics, polarity, surface charge distribution, electron - proton transfer, storage ability and the labiality of lattice oxygen. Metal ion doped HPOM materials are technologically important due to its high electrical and thermal conductivities [1-7]. The heteropolyanions of V, Mo, and W find applications in biochemical industrial catalysis, proton conductors [8], ion exchange materials, thin layer chromatography, materials for separation of amino acids [9]. Heteropolyoxometalates

*Corresponding author: sambhaji_mane@rediffmail.com

(HPOM), in addition to their considerable applications in catalysis and medicine, are attracting attention as compounds for advanced materials due to their antiviral, anti-HIV activity and potential applications in opto-electronic devices [10, 11]. The most advantageous feature of HPOM is that nearly every molecular property can be altered under defined conditions during the synthesis. In the present investigation, we are reporting "Influence of Tl^+ doping on opto-structural and electrical properties of chemically grown tungsten heteropolyoxometalate thin films".

2. Experimental details

2.1 Preparation of solutions

Thin films of undoped phosphotungstic acid. $[H_3 (PW_{12} O_{40})]$ and Tl^+ doped phosphotungstic acid $[Tl_3 (PW_{12} O_{40})]$ were prepared using following precursor solutions.
a) 2.0 % solution of phosphotungstic acid. $[H_3 (PW_{12} O_{40})]$ in acetone.
b) 2.0 % aqueous solution of phosphotungstic acid $[H_3 (PW_{12} O_{40})]$.
c) 0.2 %, aqueous solution of thallous acetate (CH_3 – COO - Tl).
d) 0.1 % aqueous solution of polyacrylamide (PAM).

2.2 Preparation of Thin films

2.2.1 Thin Film Deposition of Undoped Phosphotungstic Acid $[H_3 (PW_{12} O_{40})]$.

For the deposition of thin films of undoped phosphotungstic acid $[H_3 (PW_{12} O_{40})]$, 2% solution of phosphotungstic acid in acetone was taken in 150 cm^3 capacity glass beaker. The cleaned and dried glass as well as FTO substrates were fitted to bakelite substrate holder and dipped in above solution. The speed of substrate rotation was kept 30 - 40 rpm. After 10 minutes the substrates were taken out of the beaker. After evaporation of acetone at room temperature there was white colored and uniform deposition of $[H_3 (PW_{12} O_{40})]$ on glass and FTO substrates. As deposited thin films were dried in constant temperature oven at 80°C. After cooling at room temperature, these films were dipped in 0.1% aqueous solution of polyacrylamide (PAM) in order to get the adhesive thin films. Thickness of the as deposited films was measured by surface profilometer and it was 508.2 nm.

2.2.2 Thin Film Deposition of Tl^+ Doped Phosphotungstic Acid $[Tl_3 (PW_{12} O_{40})]$.

90 cm^3 2 % aqueous solution of phosphotungstic acid was taken in 150 cm^3 capacity glass beaker having side arm and temperature of this solution was kept at 55°C. The clean & dry glass as well as FTO substrates were fitted to bakelite substrate holder and dipped in the 2 % aqueous phosphotungstic acid solution. After five minutes 0.2 % aqueous solution of thallous acetate was added drop wise through side arm in phosphotungstic acid solution. The speed of substrate rotation was kept 50-60 rpm. After $1^1/_2$ hour, there was white colored and uniform deposition of $[Tl_3 (PW_{12} O_{40})]$ HPOM on glass and FTO substrates. As deposited thin films were dried in constant temperature oven at 80 °C. After cooling at room temperature, these films were dipped in 0.1% aqueous solution of polyacrylamide (PAM) and again dried in constant temperature oven at 100°C in order to get the adhesive thin films. Thickness of the as deposited films was measured by surface profilometer and it was 371.8 nm.

2.3 Characterization techniques

2.3.1 SEM analysis

To observe the external morphology and average grain size of the undoped and Tl^+ doped tungsten HPOM material, as deposited thin films were annealed at 100°C for 2 hours at heating rate 10°C / min in muffle furnace. The scanning electron microphotographs of these films were

recorded on JEOL - 6360 scanning electron microscope (SEM). The average grain sizes (Ga) were determined using the linear intercept technique using following relation [12].

$$G_a = \frac{1.5L}{MN}$$

Where,

1.5 - Geometry dependent proportionality constant,
L - The total test line length,
M - Magnification,
N - The total number of intercepts.

2.3.2 AFM Study

The AFM images were recorded on JSPM-5200, in order to confirm the surface morphologies of undoped and Tl^+ doped tungsten HPOM thin films deposited by optimizing various parameters.

2.3.3 Compositional analysis by EDS

Theoretical and practical atomic percentage of phosphorus, oxygen, tungsten and thallium in the heteropolyoxometalate material was confirmed by analyzing thin films on JEOL - 6360 Energy Dispersive X-ray Analyzer.

2.3.4 Structural analysis by XRD

Thin films annealed at 100°C for 2 hours at heating rate 10°C /min in muffle furnace were analyzed by x-ray diffraction technique using Cu-K- α radiations (λ=1.5425 A°) on a PW3710/1710 PHILIPS make X-ray diffractometer. The interplaner distances d (A^0) were calculated using Bragg's law. The lattice constant (a) of the sample was determined using the relation.

$$a = d_{hkl} \sqrt{h^2 + k^2 + l^2}$$

hkl planes for different peaks in X-ray diffractogram was calculated using the relation,

$$h^2 + k^2 + l^2 = 4a^2 . \sin^2\theta / \lambda^2$$

Where,

a - Lattice constant
θ - Bragg's diffraction angle.
λ - Wavelength of X-ray;

The crystallite size of the HPOM material was determined from most intense peak (peak having 311 planes) using Debye-sheerer formula [13-17]

$$D = \frac{0.94\lambda}{\beta\cos\theta}$$

Where,

λ - Wavelength of X-ray;
β - Full width at half maximum;
θ - Bragg's diffraction angle.

2.3.5 TGA- DTA measurements

In order to check the thermal stability of undoped and Tl^+ doped tungsten HPOM material, TGA- DTA measurements were carried out in nitrogen atmosphere on TG-DTA-DSC-SDT- 2960 TA. Inc.-USA make thermogravimetric analyzer with heating rate of 10^oC /min.

2.3.6 Optical characterization

A) UV- Vis Study

In present study, UV-Visible spectrophotometer (Hitachi model 330, Japan) was used to determine absorption spectra of as deposited thin films of undoped and Tl^+ doped phosphotungstic acid in the wavelength range 350-850 nm. A glass slide of same thickness and size was used as reference throughout all the measurements. One side of the film was removed with the help of cotton swab moist in dil. HCl. The layer thickness of the as deposited samples was measured by surface profilometer. Absorption spectra was analyzed to determine absorption coefficient, optical band gap 'E_g' and mode of optical transition for undoped and Tl^+ doped phosphotungstic acid.

B) FTIR Study

Fourier transform infrared (FTIR) spectra of undoped and Tl^+ doped phosphotungstic acids were recorded from pressed KBr pellets using a Perkin-Elmer Spectrum-2000 FTIR Spectrometer.

2.3.7 Electrical resistivity measurements

The direct current (dc) electrical resistivity measurements of annealed (100^oC) thin films were done by using dc two probe method. The area of the film was defined and silver paste was applied to ensure good electrical contact to the film. The working temperature was recorded using Chromal - Alumel thermocouple. The potential drop across the film was measured with the help of Meco-801 digital multimeter and current passed through the sample was recorded with a sensitive four digit Picoammeter (Model Roorkee DPM 111).

2.3.8 Thermo electric power (TEP) measurements

Thermoelectric power measurements of annealed (100^oC) thin films were carried out under the condition of maximum temperature difference and minimum contact resistance. The temperature difference of the ends of the samples was measured with Chromel–Alumel thermocouple placed in such a way so as to touch the sample ends. The thermoelectric voltage or seebeck voltage developed across the sample and the temperature of the ends was read on Testronix microvoltmeter and Meco-801 digital multimeter respectively. A set of the values of thermoelectric voltage at various temperatures thus obtained were plotted against the respective absolute temperatures. Thermo-emf measurements have also been carried out to determine the type of conduction.

3. Results and discussion

3.1 SEM results on external morphology

In Fig. 1a and Fig.1b we present a typical scanning electron microphotographs of undoped phosphotungstic acid $H_3(PW_{12}O_{40})$ and Tl^+ doped phosphotungstic acid $Tl_3(PW_{12}O_{40})$ thin films. The microphotographs of undoped and Tl^+ doped thin films showed that, both materials are polycrystalline in nature with uniform distribution of crystallites. After doping Tl^+ the average grain size decreases and spherical shaped grains are formed. The average grain size (Ga) of

undoped and Tl^{+} doped tungsten HPOM calculated by linear intercept technique was found to be 289 nm and 127 nm respectively.

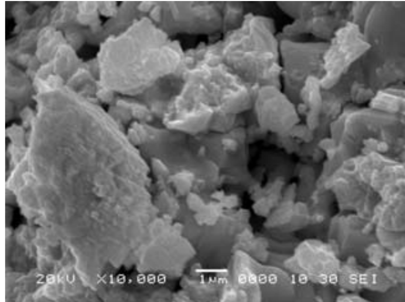

Fig. 1a SEM image of PTA [$H_3 (PW_{12} O_{40})$]

- **The average grain size (Ga) of PTA is 289 nm.**

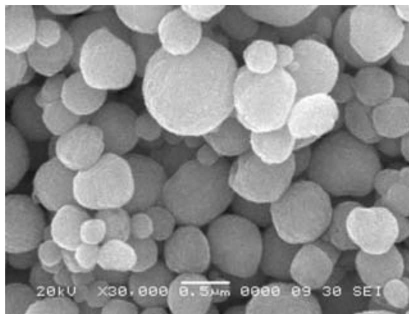

Fig. 1b SEM image of Tl PTA [$Tl_3 (PW_{12} O_{40})$] thin

- **The average grain size (Ga) of $Tl_3 (PW_{12} O_{40})$ is 127 nm.**
- **Spherical shaped**

3.2 AFM study

The AFM images were recorded in order to confirm the surface morphologies of tungsten heteropolyoxometalate thin films deposited by optimizing various parameters. A quantitative method to examine the surface morphology and structure is obtained by analyzing the surface roughness using AFM. Fig.2a and Fig.2b shows 2D and 3D AFM images of undoped and Tl^{+} doped tungsten HPOM thin films. AFM study shows films are uniform and roughness free.

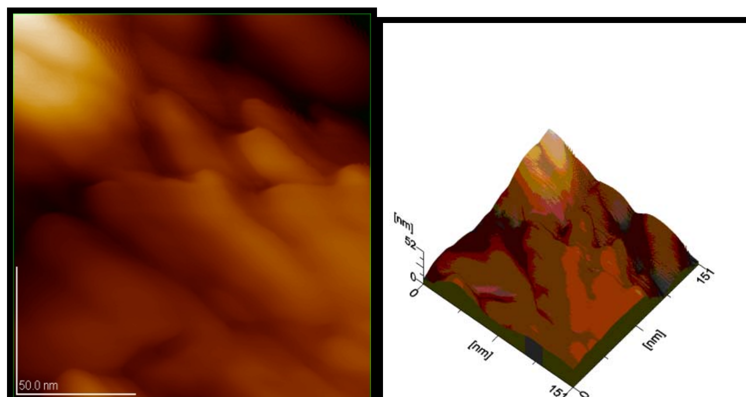

Fig.2 A_1 2D AFM image of thin film *A_2 3D AFM image of PTA*

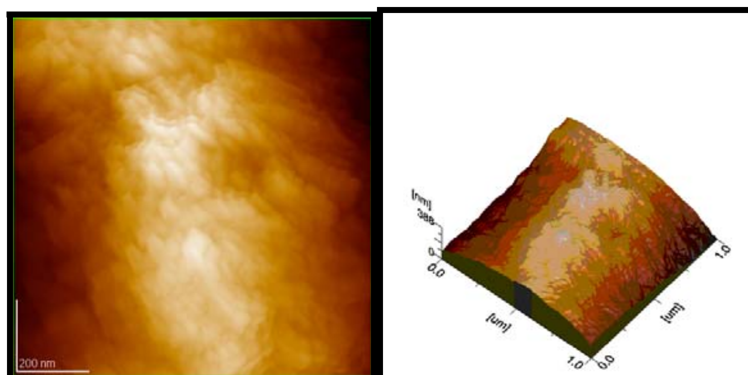

Fig.2 B_1 2D AFM image of Tl PTA thin film B_2 3D AFM image of Tl PTA

3.3 EDS results on compositional analysis

Theoretical and practical atomic percentage of phosphorus, tungsten, oxygen and thallium in tungsten HPOM sample was confirmed by analyzing annealed thin films on JEOL - 6360 Energy Dispersive X-ray Analyzer. In Fig.3a and 3b we present EDS spectra of undoped and Tl^+ doped tungsten HPOM. The EDS patterns show the presence of P, W, O and Tl in the films without any major impurity. Table 1 shows theoretical and practical atomic percentage of P, W, O and Tl. From Table 1 it is found that, in Tl^+ doped tungsten HPOM theoretical and practical atomic percentages are in good agreement.\

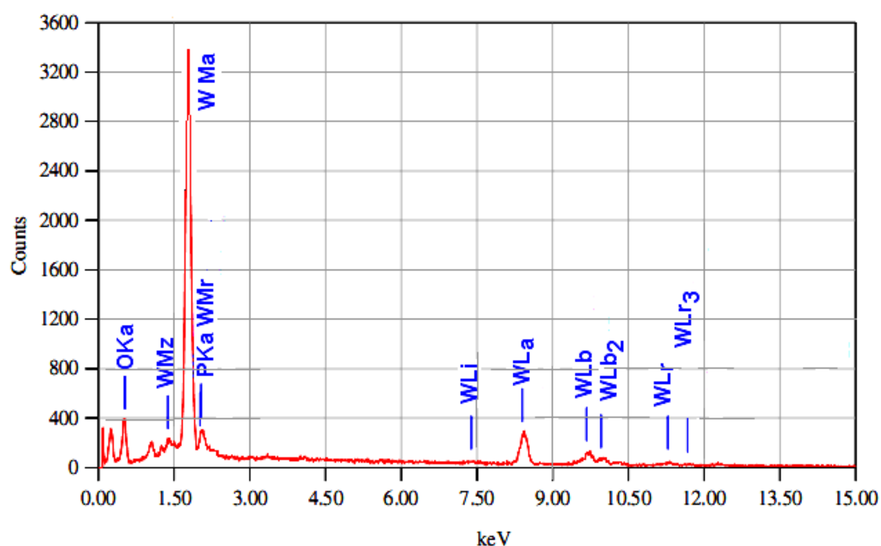

Fig. 3 a EDS of phosphotungustic acid (PTA) thin film.

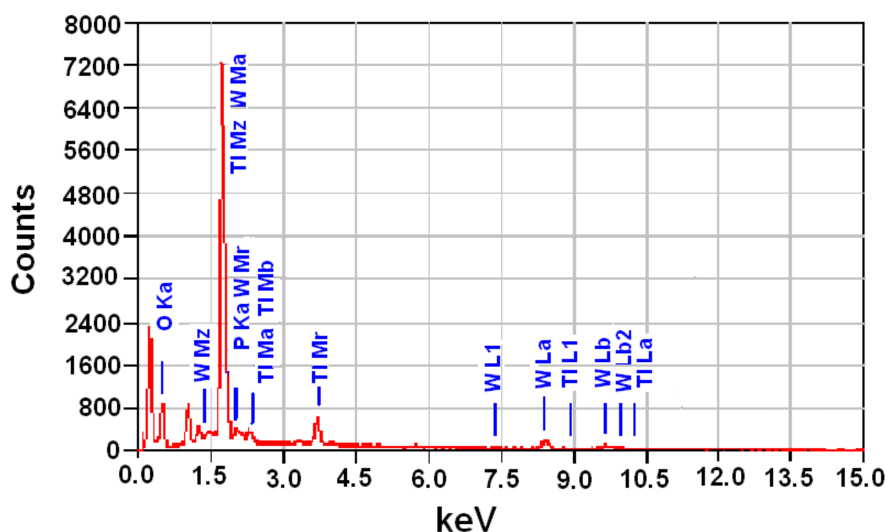

Fig. 3 b EDS of Tl^+ doped phosphotungustic acid (Tl PTA) thin film.

Table 1. Compositional analysis of Tl_3 (PW_{12} O_{40}) by EDS

Element	Theoretical Atomic %	Practical Atomic %
O	71.43	69.23
P	1.78	1.14
W	21.43	25.49
Tl	5.36	4.14

The reactions involved during the growth of tungsten HPOM thin films are

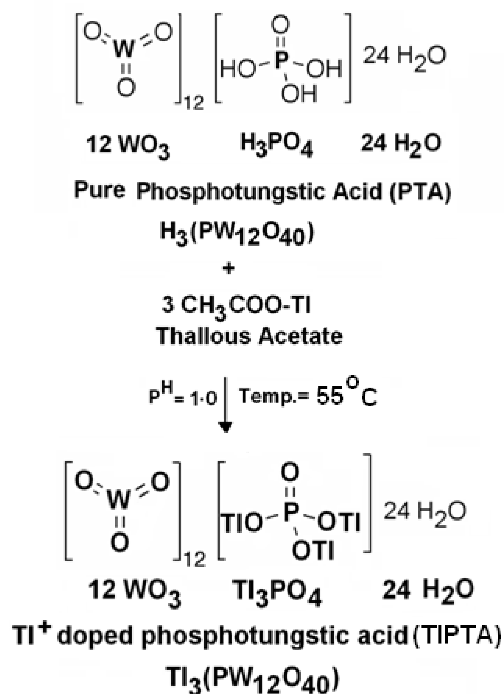

3.4 XRD Measurements

The X-ray diffractograms of undoped phosphotungstic acid and Tl^{+} doped phosphotungstic acid thin films annealed at 100°C temperature are presented in Fig. 4. The presence of planes (110), (210), (221), (311), (321), (420), (422), (520), (531) (620), (631), (642), (731), in the XRD pattern of the sample shows that the material is polycrystalline in nature with simple cubic spinel structure. The crystallite size (D) of undoped phosphotungstic acid is 29.36 nm. The crystallite size (D) of the Tl^{+} doped phosphotungstic acid is 14.16 nm. The calculated and observed values of interplaner distances are in good agreements which are tabulated in Table 2. The values of lattice constant (a) are 11.60 and 11.18 A° for undoped phosphotungstic acid and Tl^{+} doped phosphotungstic acid respectively. It is found that, after doping Tl^{+}, intensity of prominent peak (311) increases and other peaks are suppressed, indicating intercalation of Tl^{+} in the octahedral lattice of phosphotungstate anion without change in crystal structure. [13-17]. It is also found that, after Tl^{+} doping crystallite size(D), lattice constant(a) values decreases which are compared in Table 3.

Table 2. $d_{obs.}$ and $d_{cal.}$ for Tl PTA.

Sr. No.	hkl planes	$d_{observed}$ (A°)	$d_{calculated}$ (A°)
1	(110)	8.2485	8.2448
2	(210)	4.7572	4.7550
3	(221)	3.6875	3.6858
4	(311)	3.3618	3.3602
5	(321)	2.9056	2.9043
6	(420)	2.4838	2.4826
7	(422)	2.2873	2.2863
8	(511)	2.1243	2.1233
9	(520)	2.0621	2.0611
10	(531)	1.8889	1.8881
11	(620)	1.7566	1.7558
12	(631)	1.6520	1.6512
13	(642)	1.4814	1.4807
14	(731)	1.4359	1.4352

Table 3. Effect of Tl^{+} doping on crystallite size, lattice constant and average grain size

S ample	Crystallite Size, 'D' (nm)	Lattice constant, 'a' (A°)	Average grain size 'Ga' nm
[H_3 (PW_{12} O_{40})] PTA	29.36	11.60	289
[Tl_3 (PW_{12} O_{40})] Tl PTA	14.16	11.18	127

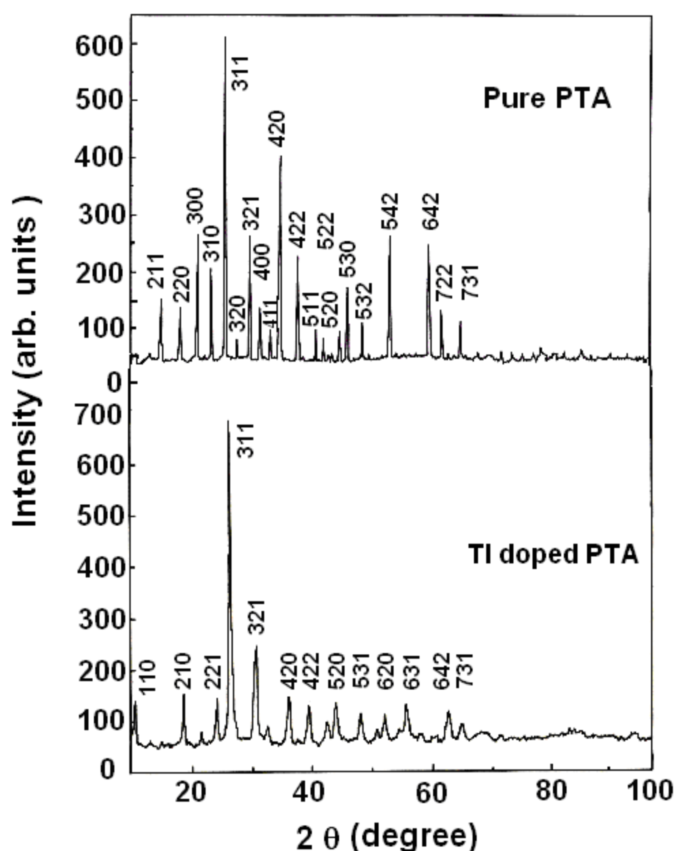

Fig. 4 XRD of phosphotungstic acid (PTA) and Tl^+ doped phosphotungstic acid(TlPTA) thin films.

3.5 TGA – DTA measurements

Thermal stabilities of undoped phosphotungstic acid and Tl^+ doped phosphotungstic acid thin films were determined by TGA-DTA measurements. Fig.5 a shows the TGA and DTA curves for undoped phosphotungstic acid. For undoped phosphotungstic acid endothermic peaks were observed at 60.88, 179.70, 478.97, 585.33, 657.21 ^{o}C,and exothermic peaks were observed at 105.86, 277.99, 566.99, 593.6, 968.45 ^{o}C on the DTA curve. From the TGA curve, three weight loss regions could be observed at 76.41, 147.49, and 428 ^{o}C for undoped phosphotungstic acid. Fig.5 b shows the TGA and DTA curves for Tl^+ doped phosphotungstic acid. For Tl^+ doped phosphotungstic acid endothermic peaks were observed at 62.12, 157.87, 433.64, 713.45^{o}C and exothermic peaks were observed at 110.86, 240.12, 556.10, 952.45^{o}C on the DTA curve. From the TGA curve, only one weight loss region could be observed at 265.12^{o}C for Tl^+ doped phosphotungstic acid. The acid form of heteropolyacid is usually obtained with large amounts of water of crystallization, and most of these water molecules are released below 100°C.Decomposition,which takes place at 350-600°C is believed to occur according to equation

$$H_3PW_{12}O_{40} \longrightarrow (1/2)\, P_2O_5 + 12WO_3 + (3/2)\, H_2O$$

Hodnett and Moffat assumed that this decomposition proceeded via $PW_{12}O_{38}$ in the case of $H_3PW_{12}O_{40}$. The thermal stability also depends on the environment. In a reducing atmosphere heteropolycompounds decompose more rapidly. The coexistence of oxygen and water vapour enhances the stability at high temperatures and sometimes causes the reformation of the heteropolystructure from a decomposed mixture. TGA-DTA curves show that, $Tl_3PW_{12}O_{40}$ material is thermally stable up to temperature 265.12 ^{o}C [18-20].

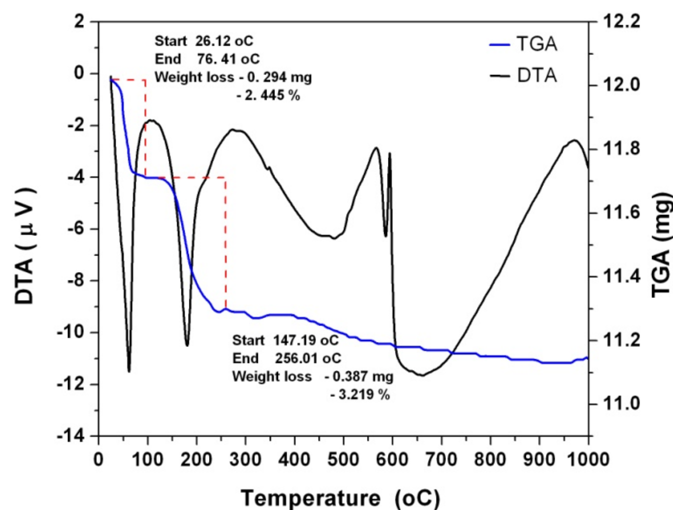

Fig.5 a TGA-DTA curves for Phosphotungustic acid (PTA).

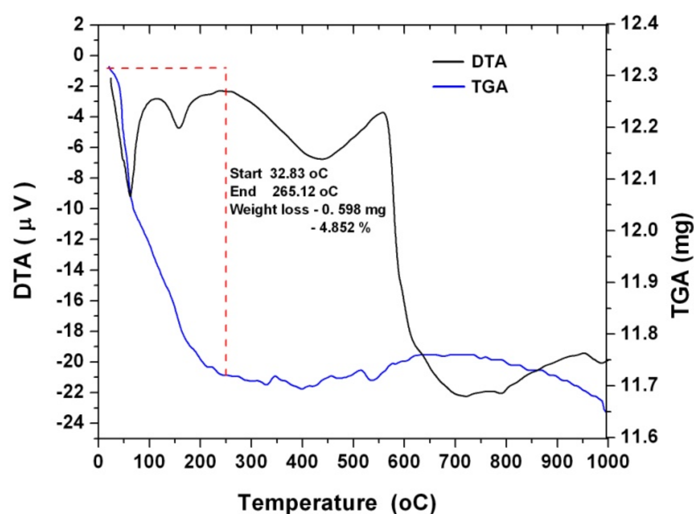

Fig.5 b TGA-DTA curves for Tl^+ doped Phosphotungustic acid(TlPTA).

3.6 Optical property es

A) UV-Visible

The optical absorption coefficient of undoped phosphotungstic acid and Tl^+ doped phosphotungstic acid thin films was calculated using the absorbance values measured for a particular wavelength (λ) and film thickness (t) using the relation

Absorption Coefficient (α) = Optical density / Thickness (t)

Thickness of the film was measured on surface profilometer. The optical band gap (Eg) was found graphically from the calculated values of the absorption coefficient (α). Fig. 6 shows the plot '$(\alpha h\upsilon)^2$' versus 'hυ' for undoped phosphotungstic acid and Tl^+ doped phosphotungstic

acid thin films. The presence of single slope in the curves suggests that films are of single phase in nature and the type of transition is direct and allowed. It was found that the optical band gap (E_g) decreases from 3.4 eV to 2.7 eV after Tl^+ doping [21-23].

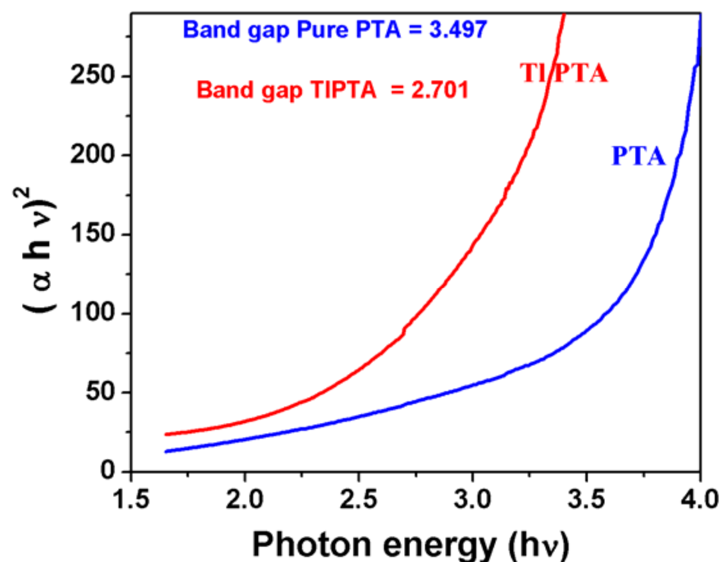

Fig. 6 Plot of $(\alpha h\nu)^2$ versus $h\nu$ for PTA and Tl^+ doped PTA thin films.

B) FTIR Study

Fourier transform infrared (FTIR) spectra of undoped phosphotungstic acid and Tl^+ doped phosphotungstic acid were recorded from pressed KBr pellets using a Perkin-Elmer Spectrum-2000 FT-IR Spectrometer. Fig. 7a and Fig. 7b shows FTIR spectra of undoped phosphotungstic acid and Tl^+ doped phosphotungstic acid respectively.

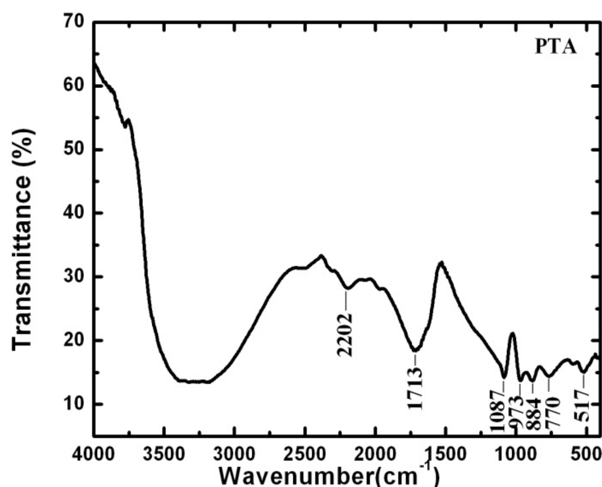

Fig. 7.a FTIR Spectra of PTA.

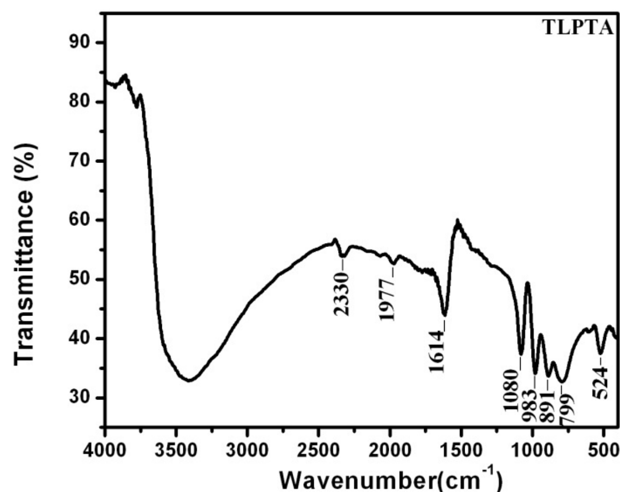

Fig. 7.b FTIR Spectra of TlPTA.

The symmetric and asymmetric stretching of the different kinds of W-O bonds are observed in the following spectral regions: W-Od bonds (1080-983cm^{-1}), W-Ob-W bridges (inter bridges between corner-sharing octahedra) (983-891cm^{-1}), W-Oc-W bridges ("intra" bridges between edge-sharing octahedra, (891-799 cm^{-1}). Only the W-Od stretching can be considered as pure vibrations: the stretching involving Ob or Oc atoms present some bend character. In our study, the IR spectrum of the present compounds exhibits the characteristic frequencies of structure in the range 1614-524 cm^{-1}. Frequency values (cm^{-1}) and assignment of FTIR bands observed for the undoped phosphotungstic acid and Tl^+ doped phosphotungstic acid are tabulated in Table 4. After doping thallium the bands arising from the HPOM change obviously either in intensity, or in position. The strong band at 3303 cm^{-1} this band was observed in all of the IR spectra. It is assigned to the water molecules involved in hydrogen bond interactions with HPOM [18, 24, and 25].

Table 4. Frequency values (cm^{-1}) and assignment of FTIR bands observed for the PTA and TLPTA

Assignment	**Frequency values (cm^{-1}) PTA [$H_3(PW_{12}O_{40})$]**	**Frequency values (cm^{-1}) TLPTA [$Tl_3(PW_{12}O_{40})$]**
W-O-W ν_1	770	799
W-O-W ν_2	884	891
W = O	973	983
P-O	1087	1080

3.7 Electrical resistivity of Tungsten HPOM thin films

The dc electrical resistivity (ρ) was measured as a function of temperature in the range 27 to 300 ^oC for polycrystalline thin films of undoped phophotungstic acid and Tl^+ doped phophotungstic acid. The resistivity data have been analyzed to distinguish between the possible mechanisms in thin films. The plots of log ρ versus 10^3 / T for undoped phophotungstic acid and Tl^+ doped phophotungstic acid thin films is shown in Fig.8.

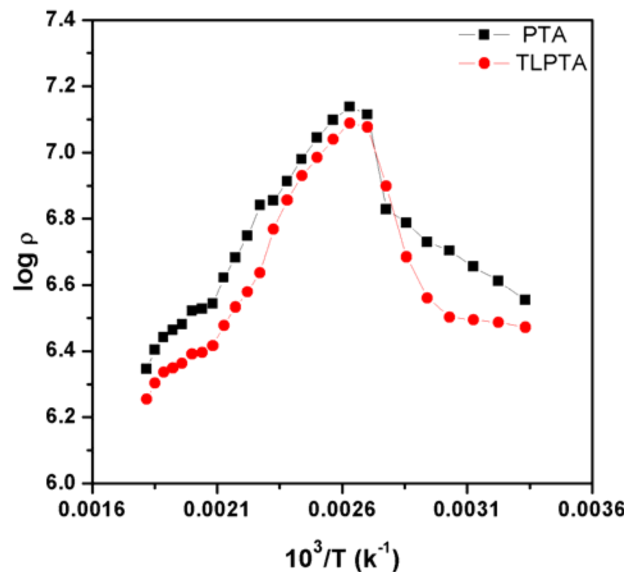

Fig. 8. Log ρ vs. 10^3 / T plots for PTA and Tl PTA thin films.

The plot of Log ρ against 10^3 / T of tungsten HPOM show that, in the lower temperature range (27 to 116 °C), both in undoped phophotungstic acid and Tl^+ doped phophotungstic acid, resistivity increases with increase in temperature indicating conducting behavior of the material. Beyond the temperature 116 °C resistivity decreases gradually. Thus the negative temperature coefficient of electrical resistivity in the temperature range 107 to 277 °C shows semiconducting nature of tungsten HPOM material and obeys Arrhenius relation.

$$\rho = \rho_0 \, e^{\Delta E / KT}$$

Where,
ρ_0 - Pre-exponential factor.
ΔE - Activation energy.
K - Boltzmann constant (8.618×10^{-5} eV/K^{-1})
T - Absolute temperature in Kelvin.

Beyond the temperature 107 °C, there are two regions namely ferrimagnetic region (107 to 277 °C) and paramagnetic region(above 277 °C). The activation energies in ferrimagnetic and paramagnetic regions are calculated from the slope of the plot Log ρ against 10^3 / T and are tabulated in Table.5

Table 5. Observed variation of ΔE for tungsten HPOM thin films

Sample	Temperature range for conducting region in K	Temperature range for semiconducting region in K
$[H_3 (PW_{12} O_{40})]$ PTA	300 -389	389- 550
$[Tl_3 (PW_{12} O_{40})]$ TlPTA	300-380	380-550

Table 6. Effect of Tl^+ doping on conducting and semiconducting nature of PTA and TlPTA

Sample	Low temperature region (Ferrimagnetic) ΔE (eV)	High temperature region (Para magnetic) ΔE (eV)
PTA	0.23	0.58
TlPTA	0.29	0.63

From Table 6 it is observed that activation energies of PTA and Tl PTA, in the paramagnetic region is found to more than that for the ferrimagnetic region. This can be attributed to the effect of magnetic ordering in the conduction process. From resistivity plot, it is also observed that resistivity of TlPTA is lower than that PTA. This is due to lower concentration of hopping mechanism due to anions [26-30].From resistivity data it is also observed that room temperature resistivity of PTA is 3.58×10^6 Ωcm and TlPTA is 2.95×10^6 Ωcm.

3.8 Thermoelectric power (TEP) of tungsten HPOM thin films

Thermoelectric power (TEP) is the most sensitive to any change or distortion of the Fermi level in the material. The temperature difference between the ends of sample causes transport of carriers from hot to cold end and thus creates electrical field which gives rise to thermal voltage. This thermally generated voltage is directly proportional to the temperature difference created across the semiconductor. Seebeck coefficient (thermopower) of a thin film was determined from the plot of the measured Seebeck voltage versus the temperature difference across the specimen ($S = \Delta V/\Delta T$).

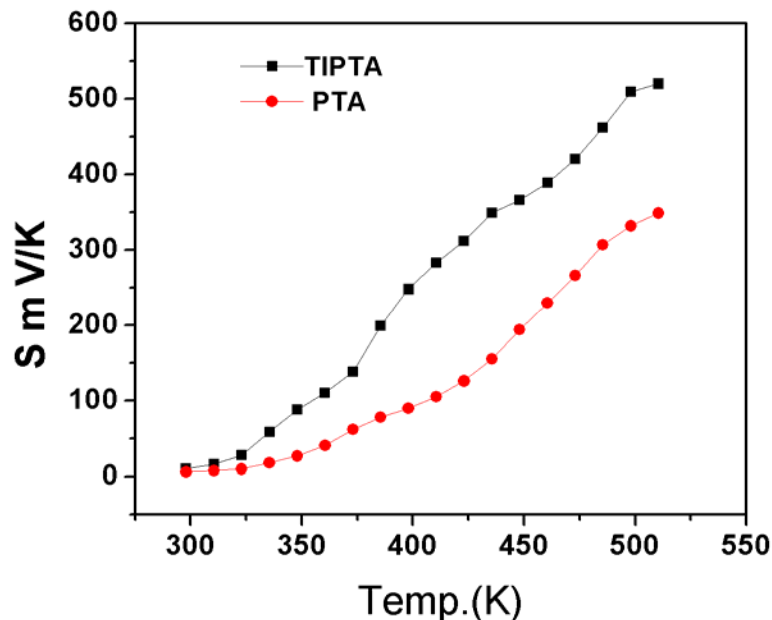

Fig. 9. Temperature dependence of the Seebeck coefficient of PTA and Tl PTA thin films

We measured the Seebeck coefficients (S) of the PTA and TlPTA in the range 300 K to 500 K and is shown in Fig.9. The Seebeck coefficient of PTA and TlPTAthin films is quite high and positive. From thermo-emf (TEP) measurements it was found that, the TEP possessing plus

sign over the whole range of temperature providing that, p-type semiconducting behavior [31] and the dominant contributing carriers are holes. The contribution of holes is thermally activated and hence the TEP increases continuously with increasing temperature.Doping of thallium in phosphotungstic acid increases hole concentration which results in increase in Seebeck coefficient [32]. Fig.9 shows that temperature dependence of thermoelectric power is approximately linear in the low temperature region, whereas it deviated from the linear behaviour at higher temperatures indicates nondegeneracy of the material whose Seebeck coefficient is a weak function of the temperature. Increase in Seebeck coefficient with increase in temperature can be attributed to the increase in concentration and mobility of the charge carrier with rise in temperature [33].

4. Conclusions

Thin films of Tl_3 (PW_{12} O_{40}) were prepared by simple chemical growth process. X-ray diffraction study confirms well formation of spherical and nanocrystalline tungsten HPOM material with simple cubic spinal structure. Band gap (Eg), crystallite size, lattice constant and resistivity of the material decreases with Tl^+ doping. Electrical resistivity and TEP study shows tungsten HPOM material is p- type semiconducting. It is also found that after doping thallium, material exhibits semiconducting behavior at lower temperature. Thus the Tl_3 (PW_{12} O_{40}) HPOM material is applicable in fabricating microelectronic and semiconducting devices.

References

[1] Ying-Hua Sun, Ji-Qing Xu, Ling Ye, Xiao-Bing Cui, Yong Li, Hai-Hui Yu, Guang-Hua Li, Guang-Di Yang and Yan Chen J. Mol., Str.**740,** 193 (2005)
[2] Laurent Lisnard, Anne Dolbecq Pierre Mialane, Jerome Marrot and Francis Secheresse J. Inorganica Chimica Acta, **357,** 845 (2004)
[3] L.Marosi, J. Cifre and C.Otero Arean J.Powder Diffraction, **18,** 236 (2003)
[4] T. Yamse. Chem. Rev., **98,** 307 (1998)
[5] Wei Feng, Tierui Zhang, Yan Liu, Ran Lu, Cheng Guan, Yingying Zhao and Jiannian Yao Mater. Chem. Phy., **77**, 294 (2003)
[6] B. Keita, L. Nadjo. J. Mat. Chem. Phy. **22** ,77 (1989)
[7] Wei Feng, Tie Rui Zang, Yan Liu, Ran Lu,Ying Ying Zhao,Tie Jin Li,and Jian Nian Yao J. Solid State Chem., **169** ,1 (2002).
[8] U. B. Mioc, M.R.Todorovic, M.Davidovic, Ph.Colomban and I. Holclajtner-Antunovic. J. Solid State Ionics, **176**, 3005 (2005).
[9] Shin-Ya Fujibayashi, Kouichi Nakayama, Masatoshi Hamamoto, Satoshi Sakaguchi, Yutaka Nishiyama and Yasutaka Ishii.J. Mol. Cat.-A: - Chemical, **110** 105 (1996).
[10] M. T. Pope, A. Muller (Eds.) Polyoxometalates: - Kluwer Academic, Dordrecht. (1994).
[11] Wang, X., J. Liu, M. T. Pope: Dalton Trans, **957** (2003).
[12] J. C. Wurst, J. A. Nelson, J.American. Ceramic. Soc., **55** 109 (1972)
[13] Klug H P, Alexander L E , X-ray diffraction procedure For Polycrystalline and Amorphous Materials, 2nd Edition. Wiley- Interscience New York, 656, (1974)
[14] B.D.Cullity, Elements of X-ray Diffraction, Addison-Wesley Publishing Company, 471, (1956)
[15] H. Hayashi and J. B. Moffat, J. Catl. **77**, 473 (1982)
[16] H. Hayashi and J.B. Moffat J Catl.,**83** ,192 (1983)
[17] B.K. Hodnett and J.B. Moffat J Catl., **88,** 253 (1984)
[18] Thanganathan Uma and Masayuki Nogami J.Chem.Mater., **19,** 3604 (2007).
[19] Uda,T.;Haile,S.M.Electrochem.SolidStateLett., **8A** ,245 (2005)
[20] Hodnett,B.K.;Moffat,J.B.J.Catal.,**88,** 253 (1984).
[21] You, W.; Wang, E.; He, Q.; Xu, L.; Xing, Y.; Jia, H. J. Mol.Struct., **524,** 133 (2000).

[22] Fu, X.K.; Chen, J.R.; Li, L.Q.; Wang, Q.; Sui, Y. Chin. Chem. Lett., **14** ,515 (2003)
[23] S.Shanmugam,B.Viswanathan ,T.K.Varadarajan Mat. Chem. and Phy., **112,** 863 (2008)
[24] Ranga Rao G and Rajkumar T Catal. Lett., **120,** 261 (2008)
[25] Ranga Rao G and Rajkumar T J. Colloid Interface Sci., **324,** 134 (2008)
[26] Z. G. Shao, P. Joghee, I. M. Hsing, J. Memb. Sci., **229,** 43 (2004)
[27] Y. S. Kim, F. Wang, M. Hickner, T. A. Zawodzinski, J. E. McGrath, J. Memb. Sci., **212**, 263 (2003)
[28] Gomez-Romero, P., M. Chojak, K. Cuentas-Gallegos, J.A. Asensio, P. J. Kulesza, N. Casan-Pastor and M. Lira-Cantu: Electrochem Com., **5**, 149 (2003)
[29] López, X., J. M. Maestre, C. Bo, J. M. Poblet J Am Chem Soc **123** ,9571,(2001)
[30] Gomez-Romero, P J. Adv Mater., **13** ,163 (2001)
[31] M.Morsli, A.Bonnet and A Conan, J. Phys.Rev.B, **39,** 3735 (1989)
[32] A.H.Abou El Ela, A.Abdelghani and H.H.A. Labib.J. App.Phys.A-Mat.Sci. Processing, **27,** 161 (1982)
[33] M.M.Abd El-Raheem, J. World Applied Science, **2,** 204 (2007)